Gas-Phase Ion−Molecule Reactions of Metal−Carbide Cations MC_n^+ (M=Y and La; *n*=2, 4, and 6) with Benzene and Cyclohexane Investigated by FTICR Mass Spectrometry and DFT Calculations

Rui Zhang,* Adriana Dinca, Keith J. Fisher, Derek R. Smith, and Gary D. Willett

School of Chemistry, The University of New South Wales, Sydney 2052, Australia

Received: December 12, 2003; In Final Form: September 26, 2004

Yttrium- and lanthanum-carbide cluster cations YC_n^+ and LaC_n^+ (n = 2, 4, and 6) are generated by laser ablation of carbonaceous material containing Y_2O_3 or La_2O_3. YC_2^+, YC_4^+, LaC_2^+, LaC_4^+, and LaC_6^+ are selected to undergo gas-phase ion−molecule reactions with benzene and cyclohexane. The FTICR mass spectrometry study shows that the reactions of YC_2^+ and LaC_2^+ with benzene produce three main series of cluster ions. They are in the form of $M(C_6H_4)(C_6H_6)_n^+$, $M(C_8H_4)(C_6H_6)_n^+$, and $M(C_8H_6)(C_6H_6)_m^+$ (M = Y and La; n = 0−3; m = 0−2). For YC_4^+, LaC_4^+, and LaC_6^+, benzene addition products in the form of $MC_n(C_6H_6)_m^+$ (M = Y and La; n = 4, 6; m = 1, 2) are observed. In the reaction with cyclohexane, all the metal−carbide cluster ions are observed to form metal−benzene complexes $M(C_6H_6)_n^+$ (M = Y and La; n = 1−3). Collision-induced-dissociation experiments were performed on the major reaction product ions, and the different levels of energy required for the fragmentation suggest that both covalent bonding and weak electrostatic interaction exist in these organometallic complexes. Several major product ions were calculated using DFT theory, and their ground-state geometries and energies were obtained.

Introduction

In recent decades, gas-phase ion chemistry of bare or ligated transition metal ions has attracted wide research interests owing to the importance of these ions in catalytic processes, especially in the activation of C−H or C−C bonds in alkanes, being a matter of crucial concern to the petrochemical industry.[1]

Gas-phase studies have shown that many transition metal cations can react with benzene to form a metal−ion (M^+)−benzene complex[2−6] or M^+−benzyne complex by H_2 elimination(s).[7,8] The electronic charge on the metal cation remains as an active site for further clustering reactions. For example, Sc^+−benzyne can react with benzene to form condensation products $M(C_6H_4)(C_6H_6)_n^+$ (n = 1−2).[9,10] The study of the reaction of the first row transition metal cations with cyclohexane has revealed that the early transition metal cations such as Sc^+, Ti^+, and V^+ are capable of multiple dehydrogenations to yield M^+−benzene(s) complexes.[11] Other reports on the reactions of transition metal cluster ions with benzene show that multibenzene, multinuclear complexes are formed through weak electrostatic interactons.[12−14] It is important to realize that the C−H and C−C bond activation by transition metals is manifested not only by bond cleavages but also through bond formations. Schwarz's group has reported the carbon−carbon bond formation promoted by bare lanthanide cations in the gas phase.[15,16] In other studies,[17−20] the catalytic property of transition metals has been further demonstrated in the catalytic growth of carbon nanotubes. This later study has shown a different aspect of the catalytic properties of transition metals, and in fact, transition metals have been at the focus of fullerene-based chemistry for more than a decade. Endohedral and exohedral metallofullerenes,[21] MetCars (M_8C_{12}),[22] and nanotubes[23] are some of the frontiers in transition metal chemistry today.

In general, however, most of the studies on gas-phase transition metal ion chemistry were carried out with "bare" transition metal ions, and little is known of the gas-phase reactivity of ligated transition metal ions.

Here we present our investigation on the reactivity of yttrium- and lanthanum-carbide cluster cations YC_n^+ and LaC_n^+ (n = 2, 4, and 6) toward benzene and cyclohexane. The reaction pathways are investigated by FTICR mass spectrometry, by high-resolution mass measurement, and collision-induced-dissociation (CID) experiments. Density functional theory (DFT) calculations were carried out on major product ions in order to establish plausible ground-state structures.

Experimental Section

The FTICR mass spectrometric study of gas-phase ion−molecule reactions used two different FTICR mass spectrometers. The first instrument was a Bruker spectrospin CMS-47 FTICR mass spectrometer equipped with a 4.7 T superconducting magnet, and the second was a Bruker APEX II FTICR mass spectrometer equipped with 7.0 T superconducting magnet. Due to the decommission of the first instrument during this study, the work described in this report was first carried out on the Bruker spectrospin CMS-47 FTICR mass spectrometer and later repeated and continued on the Bruker APEX II FTICR mass spectrometer. The data acquired on both instruments was very similar.

On the first instrument, the target was located inside the ICR cell and mounted on one of the trapping plates. A long pulse or Q-switched Nd:YAG laser beam (at fundamental wavelength 1064 nm) was sent into the ICR cell from the opposite end of the vacuum cart and focused onto the target. In the second instrument, a modified Bruker external MALDI source was used for the laser ablation experiment. The Nd:YAG laser beam was introduced through the MALDI nitrogen laser's pathway. Ions

* Corresponding author.

10.1021/jp0378440 CCC: $30.25
Published on Web 12/09/2004

were generated externally and transferred into the ICR cell by a series of ion transfer optics. For both instruments, the laser ablation generates a spot size less than a millimeter in diameter and the laser power is on the order of several hundreds of megawatts per square centimeter.

After ions are generated and trapped in the ICR cell, ion selection and fragmentation/reaction can be performed by a pulse program complied by the Bruker software XMASS 4.0. The target was made from pyrolyzed Koppers coal-tar pitch mixed with Y_2O_3 or La_2O_3. This material and the experimental methods have been reported earlier.[24] The reactants benzene and cyclohexane were degassed by repeated freeze−thaw cycles and introduced into the ICR cell through a heated inlet system. Both static (through molecular leak valve) and pulsed (pulse valve) gas inlet techniques were used at different times. The static gas inlet technique was used mainly in the study of gas-phase ion−molecule reactions without any fragmentation processes, and a static pressure of 9×10^{-8} mbar (ion-gauge reading − uncorrected) of the reactant was maintained during the reaction period. In the case of reaction/fragmentation experiments, the pulsed gas inlet technique was used and the reactant was introduced with a pressure burst reaching as high as 1×10^{-6} mbar. Prior to the reactant introduction, a collision gas, such as argon, was maintained at 1×10^{-9} mbar pressure in the ICR cell.

For all the reactions, a minimum delay of 100 ms was allowed for collisional cooling before the reactions took place. The calculation of the collision rate indicates that when the background pressure is at 1×10^{-9} mbar, ions within *m*/*z* range 50 to 500 Da undergo one to several collisions during this period of time and, for the majority of ions trapped in the ICR cell with less than one eV kinetic energy (tapping potential 1 V on both trapping plates), this cooling time is sufficient for ions to be thermalized.

For the collision-induced-dissociation experiments, the excitation irradiation was applied to the parent ion on-resonance with its cyclotron frequency. The on-resonance irradiation (ORI) method allows the energy applied to the selected ions to be accurately determined.[25]

The DFT calculations were carried out on a Pentium II 450 MHz personal computer with 512 MB ram. Gaussian 98W quantum chemical calculation package was used in these calculations.[26] Becke three-parameter (B3) exchange functional and the Lee−Yang−Parr (LYP) correlation functional were chosen as the calculation method combined with LanL2DZ and SDD basis sets.[27] The input and output structures were constructed and viewed by *ChemBats3D* program which is a part of the *ChemOffice* chemical drawing package.

Results and Discussion

YC_n^+ and LaC_n^+ ($n < 10$) Clusters. Figure 1a and 1b are positive-ion laser ablation FTICR mass spectra of pyrolyzed Koppers coal-tar pitch containing Y_2O_3 and La_2O_3, respectively. Both mass spectra were obtained using a short pulse (8 ns) laser ablation and they show distributions of YC_n^+ and LaC_n^+ ($n < 10$) clusters. In Figure 1a, YC_2^+ is seen as the most abundant ion, with Y^+ and YC_4^+ being the other two major ions. Small traces of YO^+, YC_3^+, and YC_6^+ are also observed in this mass spectrum. In Figure 1b, LaC_2^+ and LaC_4^+ are the most abundant ions and ions up to LaC_{10}^+ can be observed. Both La^+ and LaO^+ are observed at relatively low intensities. Some dilanthanum−carbon cluster ions such as $La_2C_4^+$ and $La_2C_6^+$ also appear in this mass spectrum.

There is a clear difference between the two mass spectra. In contrast to the lanthanum−carbon clusters, most of the yttrium−carbon cluster ions show low intensities. The largest ion that can be observed is YC_6^+. No diyttrium−carbon cluster ions are observed in this experiment. As the two spectra were acquired under the optimal laser ablation conditions (both ion intensity and the number of cluster ions were optimized), the low intensity of the yttrium−carbon cluster ions is the result of low bonding energy of the yttrium−carbon bond. The photoelectron spectroscopy (PES) data show that the yttrium−carbon bonding energy is ~40 kJ mol^{-1} lower than the lanthanum−carbon bond for diatomic molecules.[28,29]

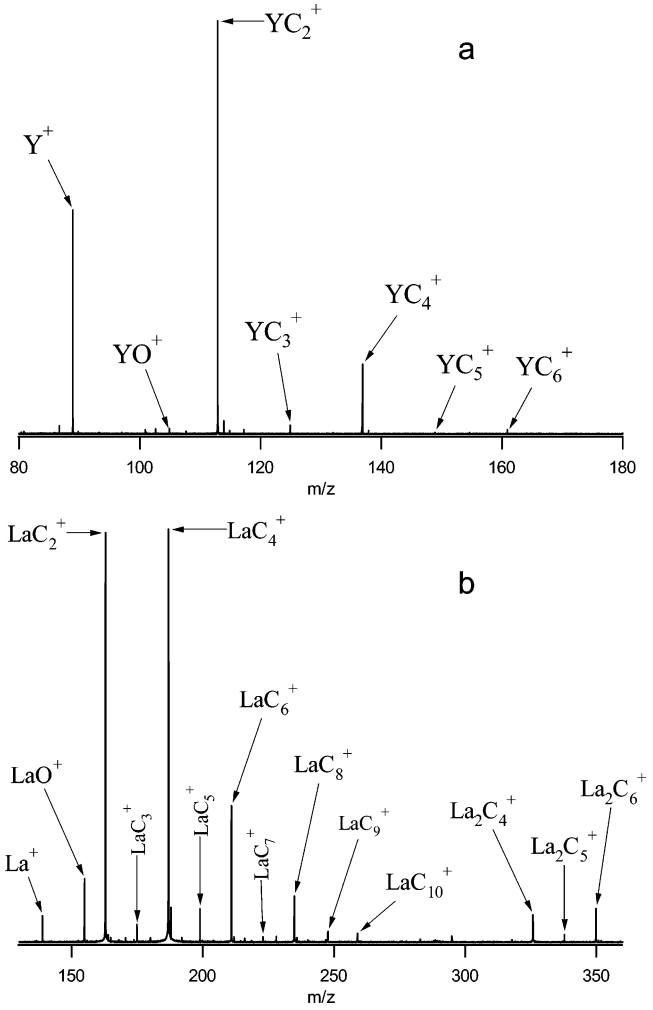

Figure 1. Positive-ion laser ablation FTICR mass spectra of pyrolyzed mixture of Koppers coal-tar pitch with (a) Y_2O_3 and (b) La_2O_3 at laser power density 500 MW cm^{-2} (8 ns, 1064 nm).

It is also obvious that the metal−carbide cluster ions containing even numbers of carbon atoms are more abundant than those with odd numbers of carbon atoms. The observed ion intensity in a laser ablation experiment can be influenced by many factors. The most important one is the ionization cross-section, which is significantly dependent on the ionization energy of each neutral species. Ayuela[30] and co-workers have reported PES studies on the electronic structure of lanthanum−carbon clusters, and they have shown that the calculated ionization potentials (IPs) for LaC_n ($n = 1-6$) versus carbon numbers show an even−odd alternation, with the IPs for the even carbon number clusters being much lower than those of the odd carbon number clusters. As the even carbon number cluster cations have a closed-shell structure and they are much more stable than their neighboring odd carbon number cluster cations, their stability is therefore reflected by their gas-phase ion abundance.

It is worthwhile to mention that the study of such metal−carbide ions is closely related to the fullerene science in the study of metallofullerenes. High-energy collision-activated-dissociation (CAD) of endohedral metallofullerene ions have shown that small metal−carbon cluster ions such as LaC_n^+ ($n < 10$) are the final fragment products in the process.[31,32] Huang and co-workers reported their study of endohedral metallofullerene formation by laser ablation of La_2O_3-doped fullerene and they found that the LaC_n^+ ($n < 8$) ions are among the products in addition to metallofullerenes.[33] Our initial observation of YC_n^+ and LaC_n^+ was also made during the study of metallofullerene formation by laser ablation. As we reported earlier, small LaC_n^+ were the major product ions for the short-pulse (8 ns) laser ablation while the long-pulse laser (230 μs) is more advantageous for metallofullerene formation.[24] We can speculate from these studies that small metal−carbides are possibly the basic building blocks for large metal−carbon clusters such as MetCars (M_8C_{12}) or as the starting unit for metallofullerenes. The critical factor that determines whether MetCars or metallofullerenes are formed is the metal-to-carbon ratio in the laser ablation targets.

Reactions of YC_n^+ and LaC_n^+ with Benzene and Cyclohexane. As YC_n^+ and LaC_n^+ are isovalent species, the reactions of YC_n^+ with benzene are expected to be very similar to the reactions of LaC_n^+ with benzene. The experimental results show almost identical reaction pathways for the two types of cluster ions. For simplicity of presentation, the reactions with LaC_n^+ will be discussed as representative. It is also important to note that, in this section of discussion, ion structures indicated by the molecular formulas have not been independently confirmed. Both experimental and quantum chemical calculation methods are used to reveal these structures, which will be discussed in detail later.

LaC_2^+ is selected from the product of laser ablation and is reacted with benzene at a static pressure of 1×10^{-8} mbar. The initial product ions observed after 0.5 s elapsed reaction time are $La(C_6H_4)^+$, $La(C_8H_4)^+$, and a small amount of $La(C_8H_6)^+$. LaO^+ is also observed, presumably due to the reaction with very low level of background water (less than 1×10^{-9} mbar), YO^+ and LaO^+ are not reactive toward benzene and cyclohexane (separate experiments were performed by isolating either YO^+ or LaO^+ to react with both reagents but no product ions were observed). Except for LaO^+, the other three cluster ions $La(C_6H_4)^+$, $La(C_8H_4)^+$, and $La(C_8H_6)^+$ continue to react with benzene or background water through three main routes as shown in Figure 2.

In the reaction route I, the lanthanum−benzyne cation $La(C_6H_4)^+$ adds up to three benzene molecules and forms a series of complex cluster ions $La(C_6H_4)(C_6H_6)_n^+$, where $n = 1-3$. Small amount of these cluster ions (for $n = 0-2$) can react with background water to form $LaO(C_6H_6)_n^+$, where $n = 1-3$. With longer elapsed reaction time (over 15 s), further water addition occurs and $LaO(C_6H_6)_n(H_2O)^+$ ($n = 1-2$) are observed. In route II, $La(C_8H_4)^+$ adds up to three benzene molecules to form $La(C_8H_4)(C_6H_6)_n^+$, where $n = 1-3$, and further reactions with background water produced complex species $LaO(C_8H_6)(C_6H_6)_n^+$ ($n = 0-2$). In the reaction route III, $La(C_8H_6)^+$ adds two benzene molecules to form $La(C_8H_6)(C_6H_6)_n^+$ ($n = 1-2$). The reaction profiles of three major reaction routes are shown in Figure 3. These profiles indicate that the formation of the $La(C_8H_4)(C_6H_6)_n^+$ series is the dominant reaction route, followed by the $La(C_6H_4)(C_6H_6)_n^+$ and $La(C_8H_6)(C_6H_6)_n^+$ series. As the background water exists only at extremely low concentration as mentioned above, all the product ions involving reaction with water molecules are observed in very low abundance.

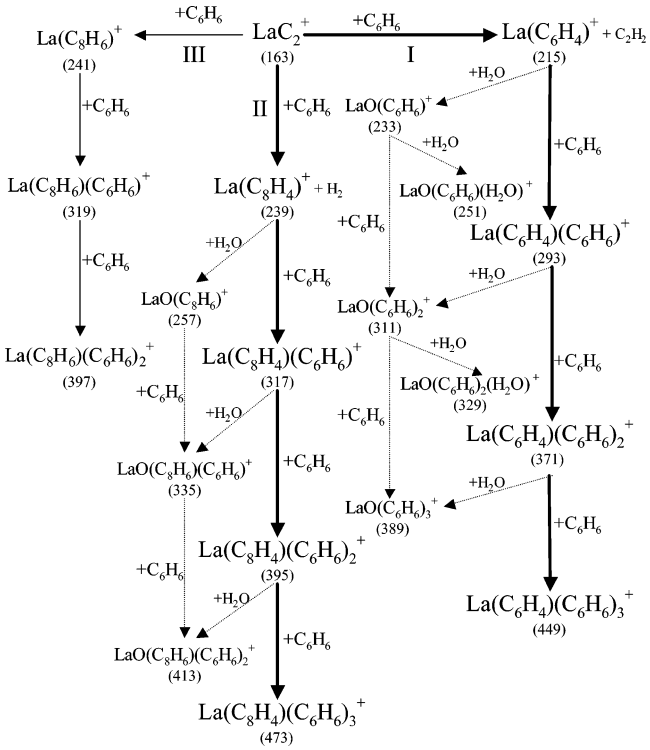

Figure 2. Reaction pathways for MC_2^+ reacting with benzene.

The reaction profiles also indicate that the reaction product ions undergo a clustering process as the reaction time extended. As these data were obtained from the reactions at a static pressure of benzene vapor less than 9×10^{-8} mbar (for the reason that low pressure is necessary for FTICR detection to have good mass resolution), the clustering process was relatively slow; no large clusters such as $La(C_6H_4)(C_6H_6)_3^+$ are observed. The clustering process can be accelerated by increasing the reactant concentration in the ICR cell. By using the pulsed gas inlet technique, the pressure of benzene vapor can be taken as high as 1×10^{-6} mbar. Under such conditions, the formation of large cluster ions such as $La(C_6H_4)(C_6H_6)_3^+$ was observed at very short reaction periods.

The clustering process has also shown a limit beyond the influence of the reaction time and reactant concentration. $La(C_6H_4)(C_6H_6)_3^+$, $La(C_8H_4)(C_6H_6)_3^+$, and $La(C_8H_6)(C_6H_6)_2^+$ are the largest ions observed in each of the three reaction routes. Increasing the reaction time or reactant concentration does not produce any larger cluster ions.

The reactions of LaC_4^+ and LaC_6^+ with benzene do not form any dehydrogenation products. Instead, benzene addition products in the form of $LaC_4(C_6H_6)_n^+$ and $LaC_6(C_6H_6)_n^+$ ($n = 1-2$) are respectively detected. Water addition products $LaC_4(C_6H_6)(H_2O)^+$ and $LaC_6(C_6H_6)(H_2O)^+$ are also observed as minor product ions. The reaction profiles of the two reactions are showing in Figure 4.

These observations suggest that LaC_2^+ may have very different electronic structure than LaC_4^+ and LaC_6^+, which results in different reactivity. If MC_n^+ has a linear structure, which is commonly agreed upon for small carbon clusters C_n ($n < 10$),[34,35] then the extension of the carbon chain should have little effect on the reactivity of the metal ion. The weaker reactivity of MC_4^+ and MC_6^+ seems to suggest structures other than a linear one for these clusters. Consider the LaC_2^+ for which the C_2 may form a double-bond between the two carbon

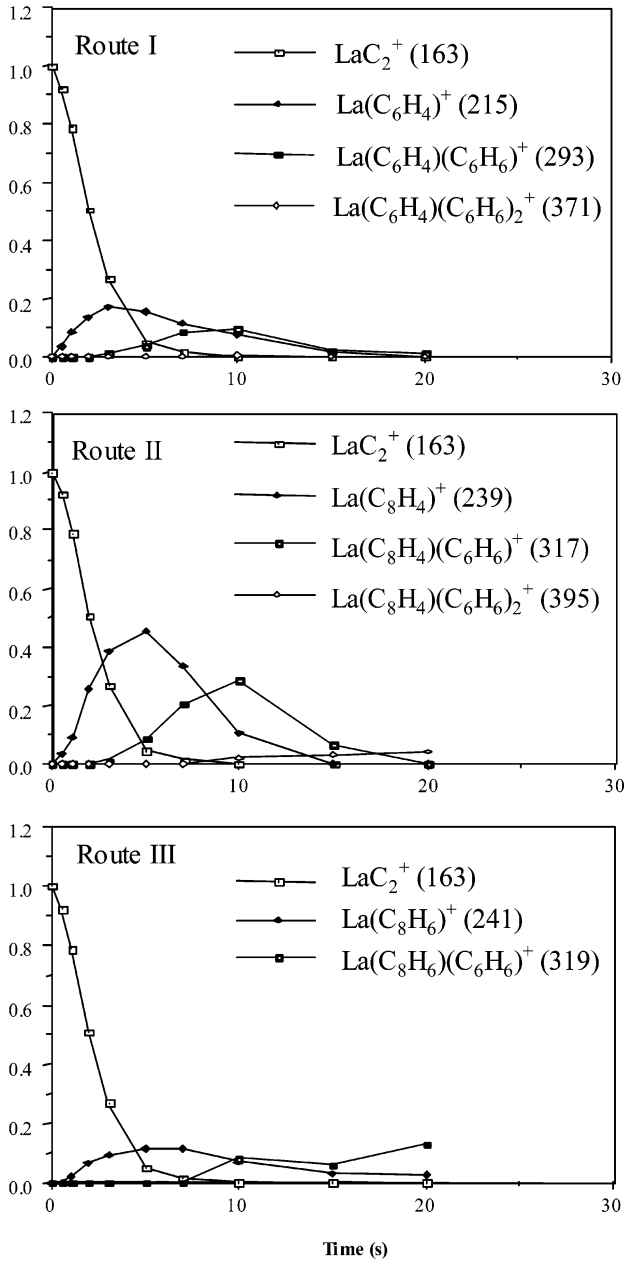

Figure 3. Reaction profile for the reaction of MC_2^+ with benzene.

atoms and the lanthanum forms a bond to each carbon; it will result a diradical cation which is a very reactive species in the gas phase. On the other hand, for LaC_4^+ and LaC_6^+, if lanthanum bonds to the carbon chain at each end, it is possible that the carbon chain has a triple bond and single bond alternation which results in a closed-shell structure for both cations.

YC_2^+ and LaC_2^+ were isolated to react with cyclohexane. In both cases, cyclohexane was dehydrogenated in several steps to yield metal−benzene complexes $M(C_6H_6)_n^+$ ($n = 1-3$ for lanthanum and $n = 1-2$ for yttrium, Figure 5).

Minor product ions such as $M(C_8H_8)(C_6H_6)_n^+$ where $n = 0-1$ were also observed, which suggested that the C_2 group in MC_2^+ was involved in the reaction. A small amount of oxygen- or water-containing species such as $MO(C_6H_6)^+$ and $M(C_6H_6)(H_2O)^+$ were also observed in both spectra. These species were presumably formed from the reaction of $M(C_6H_6)^+$ with background water. Both LaO^+ and YO^+ were also observed in the spectra, but both reactions began with only the isolated metal−carbide ion. In the reaction with MC_4^+, cyclohexane was

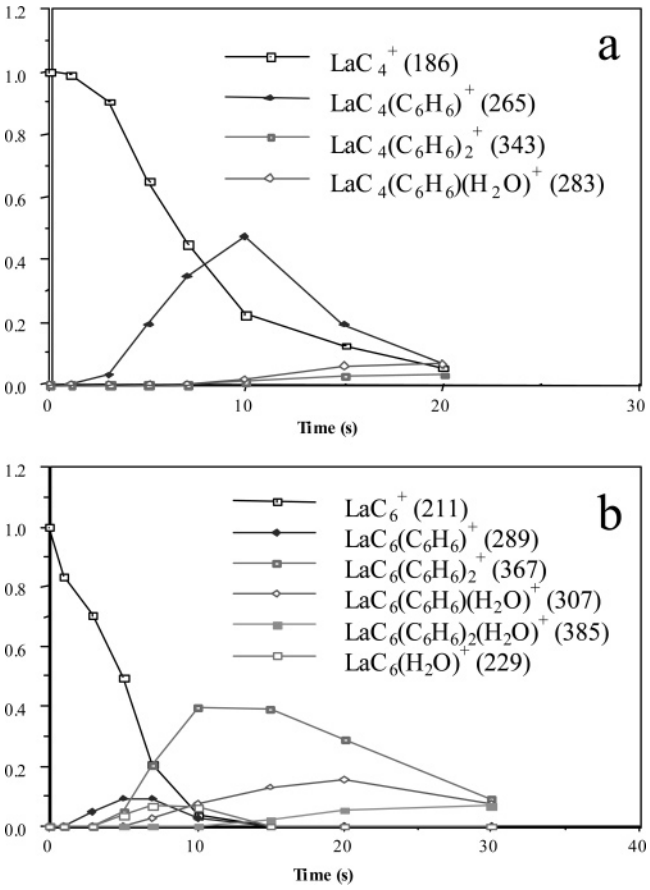

Figure 4. Reaction profile for the reaction of (a) MC_4^+ and (b) MC_6^+ with benzene.

aromatized with MC_4^+ remaining intact. $MC_4(C_6H_6)_n^+$ ($n = 1-2$) were also observed as minor product ions.

The result of the reactions of YC_2^+ and LaC_2^+ with cyclohexane seems to confirm the speculation that LaC_2^+ has a different electronic structure than LaC_4^+ and LaC_6^+. The loss of the C_2 unit from the LaC_2^+ in the reaction with cyclohexane can be explained as a diradical cation producing a neutral species − either ethene or ethane through the multiple dehydrogenation steps and left a lanthanum cation with the dehydrogenated cyclohexane. In the reaction with benzene, however, LaC_2^+ removed only two hydrogen atoms from benzene, and the further reaction involves rearrangement between $LaC_2H_2^+$ and benzyne. For LaC_4^+ and LaC_6^+, being a closed-shell structure, the dehydrogenation of cyclohexane does not involve the carbon ligands, and as a result, the carbon ligand remains intact through the reaction.

Collision-Induced-Dissociation of Ion−Molecule Reaction Products. Reactions of YC_n^+ and LaC_n^+ with benzene and cyclohexane have raised many questions about the nature of the interactions between the transition metal ion and the reactant molecules. The primary mass spectrometry results for the reactions can provide little structural information on the product ions if only the mass measurement is performed. More sophisticated mass spectrometry experiments such as collision-induced-dissociation (CID) are needed to reveal their structures.

As shown earlier, in the reaction of MC_2^+ with benzene, three series of product ions are observed. However, the formulas assigned for these product ions, in some cases, can have different interpretations with regard to their molecular structures. For example, the core ion in the $M(C_8H_6)(C_6H_6)_n^+$ series, $M(C_8H_6)^+$,

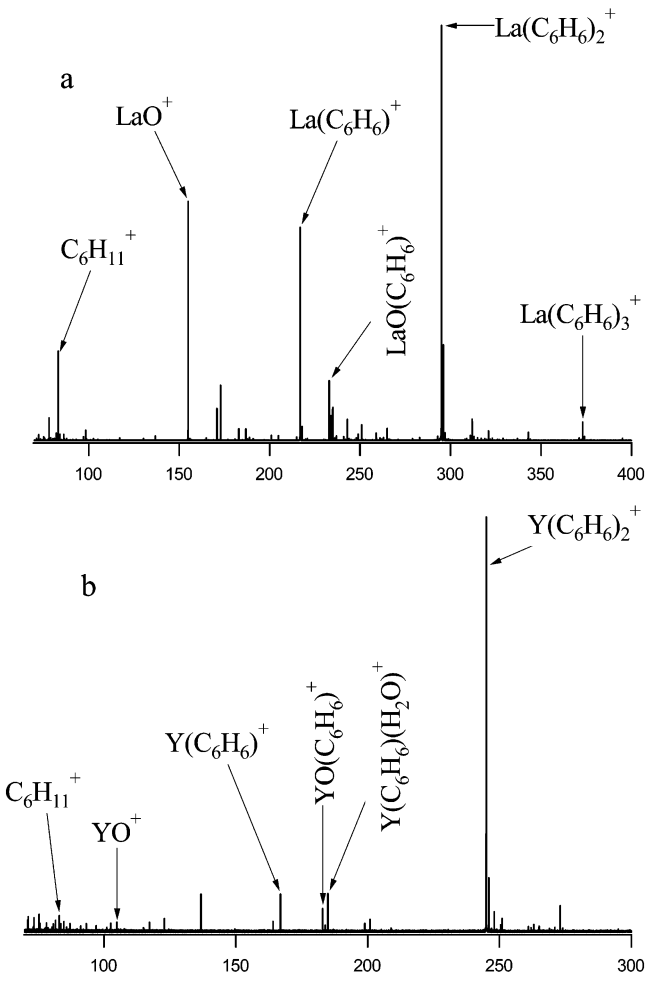

Figure 5. Positive-ion FTICR mass spectra of (a) YC_2^+ reacted with cyclohexane and (b) LaC_2^+ reacted with cyclohexane after 10 s of reaction period.

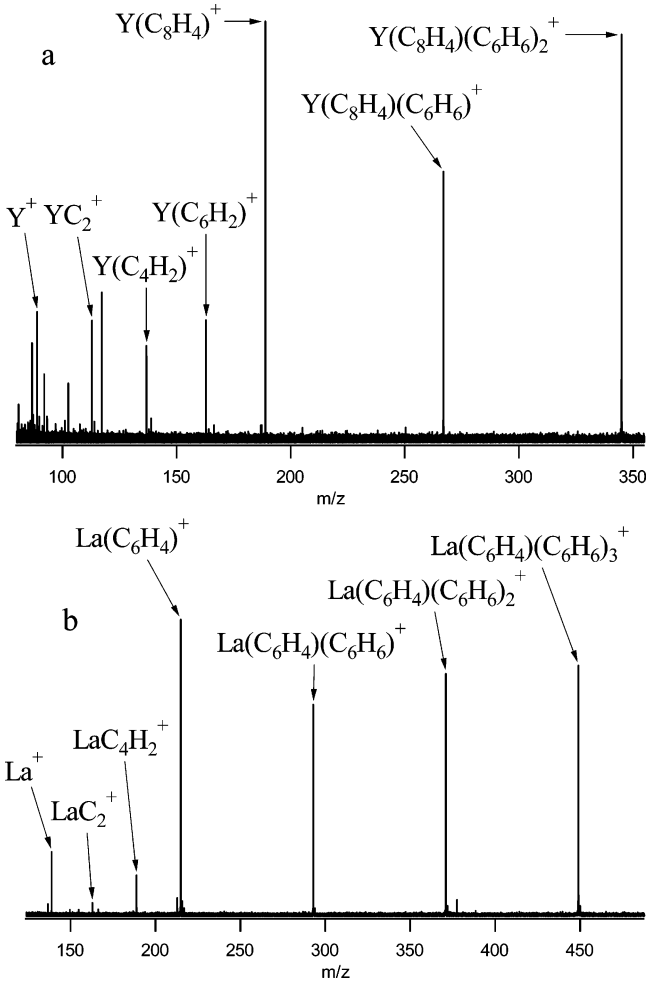

Figure 6. Positive-ion CID-FTICR mass spectra of (a) $Y(C_8H_6)(C_6H_6)_2^+$, (b) $La(C_6H_4)(C_6H_6)_3^+$.

TABLE 1: List of the CID Results for Major Reaction Product Ions

parent ion (*m*/*z*)	fragment ions from CID experiments[a]
$Y(C_8H_4)(C_6H6)_2^+$ (345)	**$Y(C_8H_4)(C_6H_6)^+$**, **$Y(C_8H_4)^+$**, $Y(C_6H_2)^+$, YC_4^+, YC_2^+, Y^+
$La(C_6H_4)(C_6H_6)_3^+$ (449)	**$La(C_6H_4)(C_6H_6)_2^+$**, **$La(C_6H_4)(C_6H_6)^+$**, **$La(C_6H_4)^+$**, $LaC_4H_2^+$, LaC_2^+, La^+
$La(C_8H_4)(C_6H_6)_2^+$ (395)	**$La(C_8H_4)(C_6H_6)^+$**, **$La(C_8H_4)^+$**, $LaC_6H_2^+$, LaC_4^+, LaC_2^+, La^+
$La(C_8H_4)(C_6H_6)^+$ (317)	**$La(C_8H_4)^+$**, $La(C_6H_2)^+$, LaC_4^+, LaC_2^+, La^+
$LaC_4(C_6H_6)_2^+$ (343)	**$LaC_4(C_6H_6)^+$**, **LaC_4^+**, LaC_2^+, La^+
$YC_4(C_6H_6)_2^+$ (293)	**$YC_4(C_6H_6)^+$**, **YC_4^+**, YC_2^+, Y^+
$La(C_8H_6)(C_6H_6)^+$ (319)	**$La(C_8H_6)^+$**, $La(C_6H_4)$+, $LaC_4H_2^+$, LaC_2^+, La^+
$Y(C_8H_6)(C_6H_6)^+$ (269)	**$Y(C_8H_6)^+$**, $Y(C_6H_4)^+$, $YC_4H_2^+$, YC_2^+, Y^+
$YO(C_6H_6)_3^+$ (339)	**$YO(C_6H_6)_2^+$**, **$YO(C_6H_6)^+$**, **YO^+**, Y^+
$LaO(C_6H_6)_2^+$ (295)	**$LaO(C_6H_6)^+$**, **LaO^+**, La^+
$YO(C_6H_6)(H_2O)^+$ (201)	**$YO(H_2O)^+$**, **YO^+**, Y^+
$LaO(C_6H_6)(H_2O)^+$ (251)	**$LaO(H_2O)^+$**, **LaO^+**, La^+
$YO(C_8H_6)(C_6H_6)^+$ (285)	**$YO(C_8H_6)^+$**,**YO^+**, Y^+
$LaO(C_8H_6)(C_6H_6)^+$ (335)	**$LaO(C_8H_6)^+$**, **LaO^+**, La^+

[a] Major fragment ions are shown in bold.

can be presented as $MC_2(C_6H_6)^+$ in which MC_2^+ exits as an entity with a benzene molecule attached. The CID results from a related product ion, $Y(C_8H_6)(C_6H_6)_2^+$, show that, after the initial loss of two benzene molecules (see Figure 6a), further dissociation of $Y(C_8H_6)^+$ resulted in loss of C_2H_2 three times followed by the loss of a C_2 group. The relatively low intensity of these fragment ions indicates that these final steps are slower than the loss of the benzene molecule(s), which suggests C_8H_6 exists as a strong covalent entity in the complex.

In another example, the fragmentation of the cluster ion $La(C_6H_4)(C_6H_6)_3^+$ shows three benzene molecules lost from the parent ion, producing three highly abundant fragment ions $La(C_6H_4)(C_6H_6)_2^+$, $La(C_6H_4)(C_6H_6)^+$, and $La(C_6H_4)^+$. Further dissociation occurs with the loss of C_2H_2 twice and a C_2 group producing a bare metal cation La^+ (Figure 6b). The intensity of the fragment ions indicates different bonding strength among all the ligands in $La(C_6H_4)(C_6H_6)_3^+$. The three benzene molecules in this complex are held together by electrostatic attraction from La^+. The relatively low intensity of the fragment ions from $La(C_6H_4)^+$ suggests strong covalent interaction between La^+ and the benzyne group.

Many other complex cluster ions have also been selected to undergo fragmentation process in order to reveal their structural information. Table 1 illustrates the CID products from these complex ions. In the $La(C_8H_4)(C_6H_6)_n^+$ series, $La(C_8H_4)(C_6H_6)_2^+$ is selected. Two benzene molecules are removed from the parent ion and produce $La(C_8H_4)^+$ in high abundance. Further dissociation showed $La(C_8H_4)^+$ loses two C_2H_2 groups and two C_2 groups. This CID result also indicates that C_8H_4 exists as an entity in the complex.

Among the LaC_4^+ reaction products, $LaC_4(C_6H_6)_2^+$ is selected for the CID experiment. Two benzene molecules are lost from this ion followed by two losses of C_2 to yield La^+. The CID result for $YC_4(C_6H_6)_2^+$ shows a very similar dissocia-

tion pattern which produces $YC_4(C_6H_6)^+$, YC_4^+, YC_2^+, and Y^+. Similar comparison can also be made between $La(C_8H_6)(C_6H_6)^+$ and $Y(C_8H_6)(C_6H_6)^+$.

Many minor product ions containing oxygen are observed in the YC_n^+ and LaC_n^+ reactions. Although the quantity of these byproduct ions is insignificant compared to the mainstream benzene-containing product ions, the structural information that these ions can provide is equally important. For this reason, both YO^+ and LaO^+, plus several oxygen-containing product ions $YO(C_6H_6)_3^+$, $LaO(C_6H_6)_2^+$, $YO(C_6H_6)(H_2O)^+$, $LaO(C_6H_6)(H_2O)^+$, $YO(C_8H_6)(C_6H_6)^+$, and $LaO(C_8H_6)(C_6H_6)^+$ are selected and studied by CID experiment.

The attempted CIDs of YO^+ and LaO^+ show no fragment ions even with maximum excitation energy applied. The CID results for other species such as $M(C_6H_4)^+$ and $M(C_8H_4)^+$ indicate that the reaction with water effectively hydrogenates the C_6H_4 and C_8H_4 groups to form $MO(C_6H_6)^+$ and $MO(C_8H_6)^+$, respectively. The strong covalent bond(s) formed between the oxygen and metal ion weakens the interaction between the metal and the organic ligands. This weakening effect was shown in the CID results of $MO(C_8H_6)(C_6H_6)^+$, and in this case, after the initial loss of a benzene molecule, the following dissociation occurred with the loss of C_8H_6 as a whole unit (no intermediate products were observed), whereas in the CID of $M(C_8H_6)(C_6H_6)^+$, $M(C_8H_6)^+$, was fragmented in several steps (see Table 1) and required much higher energy to dissociate.

In the reaction of YC_n^+ and LaC_n^+ with cyclohexane, the product M^+−benzene complex $M(C_6H_6)_n^+$ ($M = Y$ and La; $n = 1-3$) and the minor product ions $M(C_8H_8)(C_6H_6)^+$ are formed, and they are not observed in the reaction with benzene. The CID of $La(C_6H_6)_2^+$ (Figure 7a) shows that after the initial loss of a benzene molecule, further dissociation of $La(C_6H_6)^+$ involves H_2 elimination(s) and produced $La(C_6H_4)^+$ and small amount of $La(C_6H_2)^+$. Further fragmentation is similar to the dissociation of $La(C_6H_4)^+$, which loses two C_2H_2 groups and a C_2 group, producing a bare metal cation La^+. Noticeably, the fragment ion La^+ is produced in relatively higher abundance in comparison with the CID results of the benzene reaction product ions such as $La(C_6H_4)(C_6H_6)_3^+$. It suggests that the metal carbon bonding in $La(C_6H_6)^+$ is weakened by the hydrogens. Some earlier reports have suggested that in $La(C_6H_6)^+$, lanthanum is bonded to the two adjacent carbon atoms on the benzene ring. The dissociation of $La(C_6H_6)^+$ can have two pathways, different from the one described above, the other dissociation channel is to have the lanthanum ion completely separated from benzene molecule and produce bare metal ion La^+. The collective result of these two processes is higher abundance of La^+ presented in the CID spectrum of $La(C_6H_6)^+$. The fragmentation of $La(C_8H_8)^+$ first produces $La(C_6H_6)^+$, and further fragmentation is identical to that of the CID of $La(C_6H_6)^+$ (Figure 7b).

DFT Calculation on the Major Ion−Molecule Reaction Products. Quantum chemical calculations on metal−carbide cluster neutrals and cations $MC_n^{0/+}$ ($M = Y$ and La; $n < 10$) have been reported by several research groups.[36−38] They claim that the ground-state structure for these clusters is the so-called 'fan" structure for which the lanthanum atom or cation bond to each carbon atom on a curved carbon chain. For cations, the singlet state was found to be the ground state. Our calculations on both linear and 'fan' isomers for LaC_n^+ ($n = 2$, 4, and 6) agree with these results, except for LaC_6^+, where we found that its ground-state structure is not co-planer but rather a "shell" shaped structure. Lanthanum forms an angle of about 25° with respect to the plane of the six carbon atoms. (Figure 8, structures a−c). Energy wise, the shell isomer is 49.8 kJ mol^{-1} lower than the planar isomer.

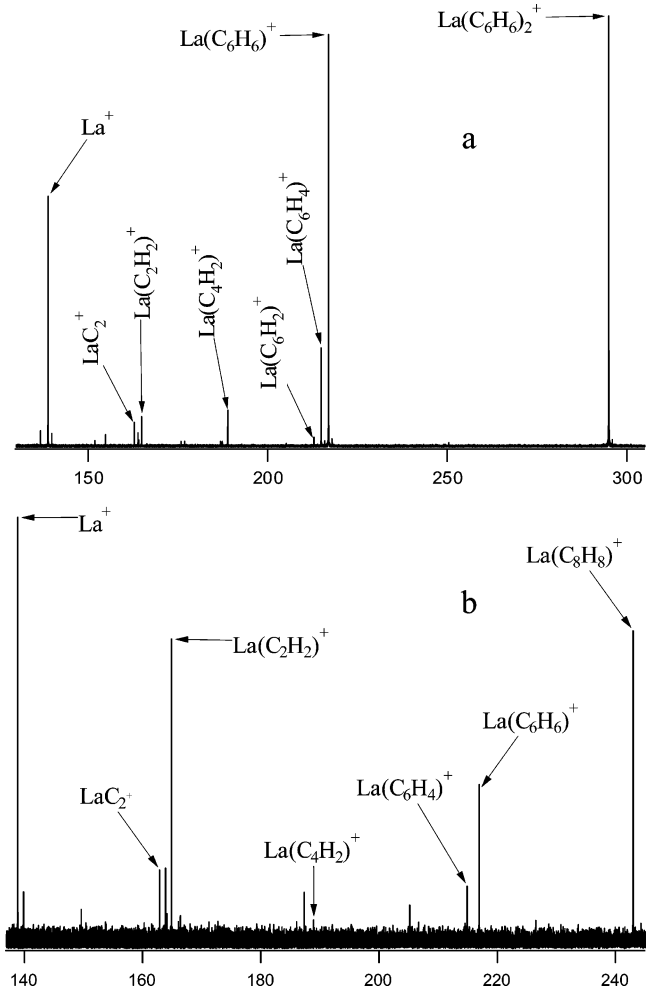

Figure 7. Positive-ion CID-FTICR mass spectra of (a) $La(C_6H_6)_2^+$, (b) $La(C_8H_8)^+$.

The calculated C−C bond length in LaC_2^+ is 1.302 Å, which is close to a double bond length. It supports the hypothesis mentioned above that LaC_2^+ behaves like a diradical cation. The calculated C−C bond lengths for LaC_4^+ and LaC_6^+ show a bond length alternation. In LaC_4^+, the two carbon−carbon bonds at each end of the chain, C_1-C_2 and C_3-C_4, have the same bond length of 1.295 Å. The C−C bond in the middle, C_2-C_3, has a bond length of 1.390 Å. In LaC_6^+, the two carbon−carbon bonds at each end of the chain, C_1-C_2 and C_5-C_6, have the same bond length of 1.286 Å. The center one C_3-C_4 is the shortest one with a bond length of 1.261 Å. The two carbon−carbon bonds in the middle, C_2-C_3 and C_4-C_5, have the same bond length of 1.383 Å.

An analysis of computed Mulliken population charges for LaC_n^+ ($n = 2$, 4, and 6) shows that the La−C bonds are strongly ionic and that the electronic charge is transferred from lanthanum to carbon atoms.[39] As the number of carbon atoms increases, the electron density on lanthanum is largely reduced, and this compromises its capability for bond activation in the ion−molecule reactions. As the result of this, only LaC_2^+ is observed to form dehydrogenation products, whereas for LaC_4^+ and LaC_6^+, mainly the addition products are observed. The La−C bond length for lanthanum−carbide cations and several cluster ions are listed in Table 2.

For $La(C_6H_4)^+$, $La(C_8H_4)^+$, and $La(C_8H_6)^+$, the energy minimal structures are obtained. As shown in Figure 8, structures

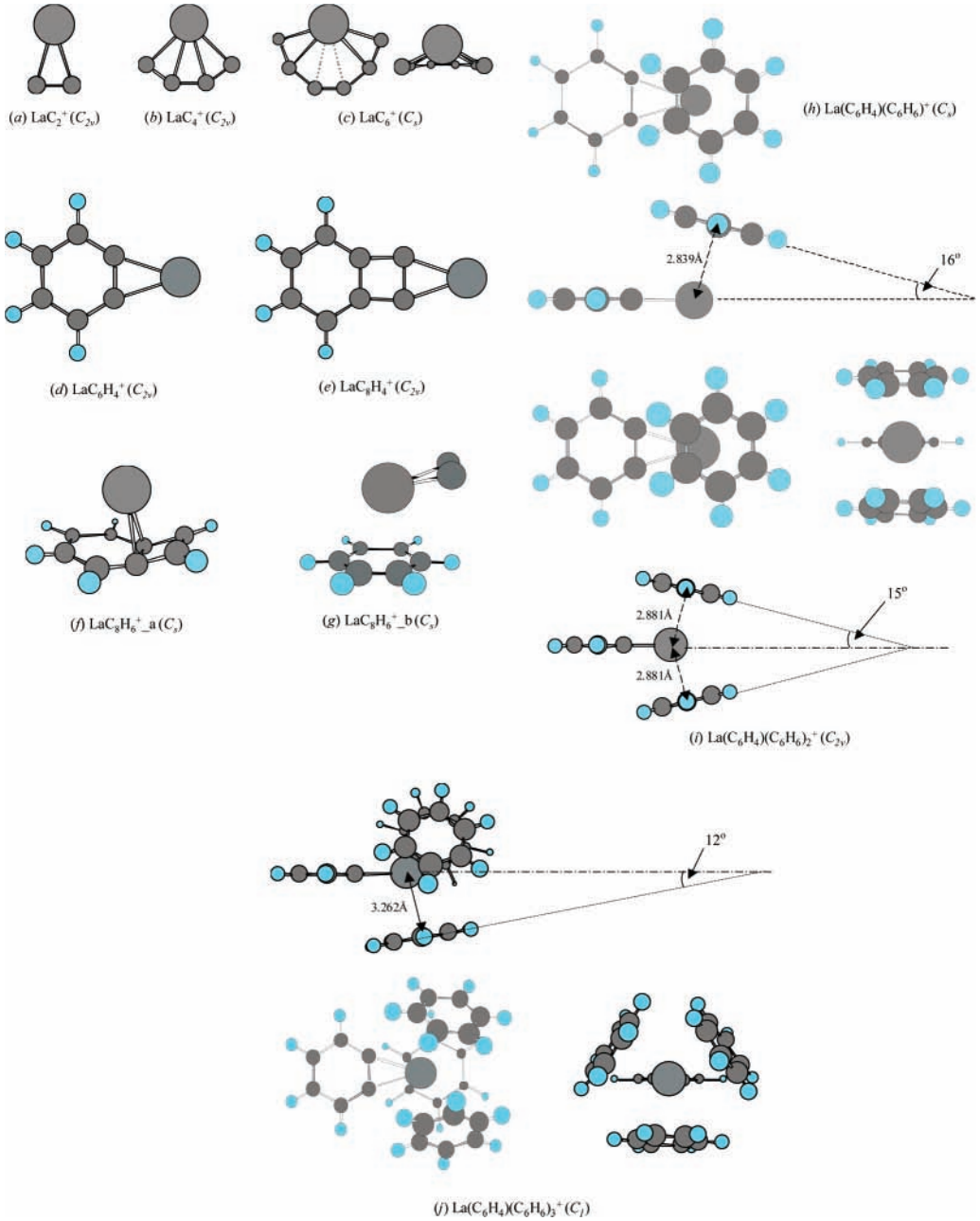

Figure 8. Fully optimized structures for LaC_n^+ and various ion−molecule reaction product ions obtained by DFT quantum chemical calculations.

TABLE 2: La−C Bond Lengths for LaC_n^+ and Major Ion−Molecule Reaction Product Ions

ions	La−C bond length (Å)
LaC_2^+	2.332
LaC_4^+	2.462 (outer), 2.576 (inner)
LaC_6^+	2.501 (outer), 2.701 (middle), 2.942(center)
$La(C_6H_4)^+$	2.315
$La(C_8H_4)^+$	2.307
$La(C_8H_6)^+$(a)	2.519
$La(C_8H_6)^+$(b)	2.345
$La(C_6H_4)(C_6H_6)^+$	2.362
$La(C_6H_4)(C_6H_6)_2^+$	2.395

d−f, in all three cases, the lanthanum cation forms two covalent bonds with their organo ligands. These structures satisfy the s^1d^1 configuration for La^+ and they have a closed-shell electronic structure, thereby making them very stable species. In the case of $La(C_8H_6)^+$, the isomer built by LaC_2^+ attached to a benzene molecule is also calculated (Figure 8, structure g). The computed result for this isomer is 149.8 kJ mol^{-1} higher than isomer structure f. This result explains the experimental observation where $La(C_8H_6)^+$ dissociates as a covalently bonded entity.

The DFT calculations also provide explanations for many of the other cluster ions. As for $La(C_6H_4)^+$ and $La(C_8H_4)^+$, the lanthanum cation is bonded with two carbon atoms away from the benzyne ring, the space that is available for further interaction is larger than $La(C_8H_6)^+$ where the lanthanum cation is blocked from one side by the ligand. As a result of the different geometries, $La(C_6H_4)^+$ and $La(C_8H_4)^+$ can add three more benzene molecules, whereas $La(C_8H_6)^+$ can add only two.

The calculations with larger cluster ions containing more than one benzene molecule prove to be very difficult because of the weak electrostatic interaction involved. The energy surface for this type of structures can be very shallow, and it is difficult to find the true global minimum. The minimal energy structure was only obtained for a very few cluster ions. The fully optimized ground-state structure for $La(C_6H_4)(C_6H_6)^+$ is shown in Figure 8 (structure h). The distance from the lanthanum cation

to the center of the absorbed benzene molecule is about 2.839 Å. The absorption angle formed between the C_6H_6 plane and the La(C_6H_4) plane is about 16°, and it has been observed during the calculation that when the two planes reach to this angle, the rotation of the benzene molecule in its plane makes very little change in the total energy. The geometry-optimized structure for La(C_6H_4)(C_6H_6)$_2^+$ shows that a "sandwich" type of structure (Figure 8, structure i) with the absorption angles between the benzene molecule and La(C_6H_4) plane at about 15°. A similar structure was initially obtained by DFT calculation for the gas-phase ion complex Sc(C_6H_4)(C_6H_6)$_2^+$ in a separate study.[40] These structures clearly show that the benzene molecules are attached to the metal cation by the electrostatic attraction, and it is this weak bonding that is responsible for the high abundance of the fragment ions observed in the CID experiments. For La(C_6H_4)(C_6H_6)$_3^+$, geometry-optimized structure is also obtained from DFT calculation (Figure 8, structure j). As the number of benzene molecules increases, the interaction between the lanthanum cation and benzene molecules becomes weaker. This effect is demonstrated by the increasing distance between the metal cation and the center of the benzene molecule(s) as shown in the Figure 8, structures h−j. An important feature of these addition products is the angle formed between the plane of the initial core-ion in each complex and the absorbed benzene molecular plane(s), and such angle is result of balancing electrostatic interactions within the complex system.

Conclusions

The study of gas-phase ion−molecule reactions of yttrium- and lanthanum-carbide cluster cations YC_n^+ and LaC_n^+ (n = 2, 4, and 6) with benzene and cyclohexane reveal ligand effect on the gas-phase reactivity of these metal−carbide cluster ions. The electron density on the metal cation is affected by the number and size of the ligands, which results in very different product ions. MC_2^+ reacts similarly to the "bare" metal cation and it is capable of dehydrogenating hydrocarbon molecules such as benzene and cyclohexane. MC_4^+ and MC_6^+ show reduced reactivity and only addition products are observed.

Collision-induced-dissociation of the complex product ions indicates that both covalent and weak electrostatic interactions are involved in the formation of these cluster ions. The clustering process is limited by the steric hindrance around the metal cation, and the largest cluster ion that can be formed depends on the available space around the core-ion in each clusters.

DFT calculation on the major product ions confirms that the "fan" structure in the singlet state is the ground-state structure for LaC_n^+ (n = 2, 4, and 6), with a modification for LaC_6^+ being a noncoplanar "shell" structure. The calculation on the complex product ions formed from LaC_2^+ indicates that C_2 can be either removed or rearranged in the product ions at the initial reaction stage. Covalently bonded structures are formed at this stage with a closed-shell electronic structure. Further addition of benzene molecules(s) onto the metal cation is stabilized by the electrostatic interactions.

Acknowledgment. This research was funded by Australian Research Council and R. Z. gratefully acknowledges a scholarship from the Australian Postgraduate Research Award (Industry).

References and Notes

(1) Eller, K.; Schwarz, H. *Chem. Rev.* **1991**, *91*, 1121−1177.

(2) Higashide, H.; Oka, T.; Kasatani, K.; Shinohara, H.; Sato, H. *Chem. Phys. Lett.* **1989**, *163*, 485.

(3) Bauschlicher, C. W.; Partridge, H.; Langhoff, S. R. *J. Phys. Chem.* **1992**, *96*, 3273−3278.

(4) Meyer, F.; Khan, F. A.; Armentrout, P. B. *J. Am. Chem. Soc.* **1995**, *117*, 9740−9748.

(5) Gibson, J. K. *J. Phys. Chem.* **1996**, *100*, 15688−15694.

(6) Gibson, J. K. *J. Alloys Compd.* **1998**, 759−764.

(7) El-Nakat, J. H.; Dance, I. G.; Fisher, K. J.; Willett, G. D. *Polyhedron* **1993**, *12*, 2477−2487.

(8) El-Nakat, J. H.; Dance, I. G.; Fisher, K. J.; Willett, G. D. *Polyhedron* **1994**, *13*, 409−415.

(9) Huang, Y.; Hill, Y. D.; Sodupe, M.; C. W. Bauschlicher, J.; Freiser, B. S. *Inorg. Chem.* **1991**, *30*, 3822−3829.

(10) Dinca, A.; Fisher, K. J.; Smith, D. R.; Willett, G. D. *Proceedings of the 16th Australian and New Zealand Society for Mass Spectrometry Conference*, 1997, University of Tasmania, Hobart.

(11) Seemeyer, K.; Schroder, D.; Kempf, M.; Lettau, O.; Muller, J.; Schwarz, H. *Organometallics* **1995**, *14*, 4465−4470.

(12) Kurikawa, T.; Takeda, H.; Nakajima, A.; Kaya, K. *Z. Phys. D* **1997**, *40*, 65−69.

(13) Yasuike, T.; Nakajima, A.; Yabushita, S.; Kaya, K. *J. Phys. Chem.* **1997**, *101*, 5360−5267.

(14) Berg, C.; Beyer, M.; Schindler, T.; Niedner-Schatteburg, G.; Bondybey, V. E. *J. Chem. Phys.* **1996**, *104*, 7940−7946.

(15) Wesendrup, R.; Schwarz, H. *Organometallics* **1997**, *16*, 461−466.

(16) Heinemann, C.; Schroder, D.; Schwarz, H. *Chem. Ber.* **1994**, *127*, 1807−1810.

(17) Birkett, P. R.; Cheetham, A. J.; Eggen, B. R.; Hare, J. P.; Kroto, H. W.; Walton, D. R. M. *Chem. Phys. Lett.* **1997**, *281*, 111−114.

(18) Seraphin, S.; Zhou, D.; Jiao, J.; Withers, J. C.; Loutfy, R. *Appl. Phys. Lett.* **1993**, *63*, 2073−2075.

(19) Guo, T.; Nikolaev, P.; Thess, A.; Colbert, D. T.; Smalley, R. E. *Chem. Phys. Lett.* **1995**, 49−54.

(20) Amelinckx, S.; Zhang, X. B.; Bernaerts, D.; Zhang, X. F.; Ivanov, V.; Nagy, J. B. *Science* **1994**, *265*, 635−639.

(21) Chai, Y.; Guo, T.; Jin, C.; Haufler, R. E.; Chibante, L. P. F.; Fure, J.; Wang, L.; Alford, J. M.; Smalley, R. E. *J. Phys. Chem.* **1991**, *95*, 7564.

(22) Castleman, A. W., Jr.; Guo, B.; Wei, S. *Clusters and fullerenes*; Kumar, V., Martin, T. P., Tosatti, E., Eds.; World Scientific: Singapore, 1992, Vol. 6.

(23) Iijima, S. *Nature* **1991**, *354*, 56−58.

(24) Zhang, R.; Achiba, Y.; Fisher, K. J.; Gadd, G. E.; Hopwood, F. G.; Ishigaki, T.; Smith, D. R.; Suzuki, S.; Willett, G. D. *J. Phys. Chem. B* **1999**, *103*, 9450−9458.

(25) Grosshans, P. B.; Marshall, A. G. *Anal. Chem.* **1991**, *63*, 2057−2061.

(26) Frisch, M. J.; Trucks, G. W.; Schlegel, H. B.; Gill, P. M. W.; Johnson, B. G.; Robb, M. A.; Cheeseman, J. R.; Keith, T. A.; Petersson, G. A.; Montgomery, J. A.; Raghavachari, K.; Al-Laham, M. A.; Zakrzewski, V. G.; Ortiz, J. V.; Foresman, J. B.; Cioslowski, J.; Stefanov, B. B.; Nanayakkara, A.; Challacombe, M.; Peng, C. Y.; Ayala, P. Y.; Chen, W.; Wong, M. W.; Andres, J. L.; Replogle, E. S.; Gomperts, R.; Martin, R. L.; Fox, D. J.; Binkley, J. S.; Defrees, D. J.; Baker, J.; Stewart, J. P.; Head-Gordon, M.; Gonzalez, C.; Pople, J. A. *Gaussian 94 (Version 3.0)*, Version 3.0 ed.; Gaussian, Inc.: Pittsburgh, PA, 1995.

(27) Becke, A. D. *J. Chem. Phys.* **1993**, *98*, 5648.

(28) Pelino, M.; Gingerich, K. A. *J. Chem. Phys.* **1989**, *93*, 1581.

(29) Shim, I.; Pelino, M.; Gingerich, K. A. *J. Chem. Phys.* **1992**, *97*, 9240.

(30) Ayuela, A.; Seifert, G.; Schmidt, R. *Z. Phys. D.* **1997**, *41*, 69−72.

(31) Lorents, D. C.; Yu, D. H.; Brink, C.; Jensen, N.; Hvelplund, P. *Chem. Phys. Lett.* **1995**, *236*, 141−149.

(32) Suzuki, S. *J. Chem. Phys.* **1990**, *93*, 4102−4111.

(33) Huang, R.; Li, H.; Lu, W.; Yang, S. *Chem. Phys. Lett.* **1994**, *228*, 111−116.

(34) Raghavachari, K.; Binkley, J. S. *J. Chem. Phys.* **1987**, *87*, 2191−2197.

(35) Martin, J. M. L.; Francois, J. P.; Gijbels, R. *J. Chem. Phys.* **1990**, *93*, 8850.

(36) Suzuki, S.; Torisu, H.; Kubota, H.; Wakabayashi, T.; Shiromaru, H.; Achiba, Y. *Int. J. Mass Spectrom. Ion Proc.* **1994**, *138*, 297−306.

(37) Strout, D. L.; Hall, M. B. *J. Phys. Chem.* **1996**, *100*, 18007.

(38) Roszak, S.; Balasubramanian, K. *J. Chem. Phys.* **1997**, *106*, 158−164.

(39) Jackson, P.; Willett, G. D.; Mackey, D. W.; van der Wall, H.; Gadd, G. E. *J. Phys. Chem. A* **1998**, *102*, 8941−8945.

(40) Dinca, A.; Fisher, K. J.; Smith, D. R.; Willett, G. D., unpublished results.